Fröhlich Resonance in Carbon Nanospiroids and the 2175 Å Interstellar Absorption Feature

Sergey Yastrebov [a], Maxim Chekulaev [a],
Alexandra Siklitskaya [b], Jacek A. Majewski [b], Roger Smith [c]

[a] *A.F.Ioffe Physicotechnical Institute, St.Petersburg, Russia*
[b] *Theoretical physics institute, Warsaw, Poland*
[c] *School of Science, Loughborough University, Loughborough, United Kingdom*

Abstract

This paper demonstrates that a free electron gas model simulates quite well the spectral dependence of optical extinction spectra for carbon spiroids both synthesised in laboratory experiment and present in the interstellar medium. The assumption was made that the free electrons are confined in an homogeneous spherical particle owing to the delocalisation of π electrons that occurs in the actual spectral range.

1 Introduction

Analysis of the optical emission spectra from the ELIAS 1 and HD97048 spacecraft, indicates the presence of small diamonds in the interstellar medium due to the emission bands at 3.43-3.53 mkm [1]. These bands are fingerprints of nanodiamonds and occur together with the emission band at 3.3 mkm that is the fingerprint of graphene [[1,2]] The size of the nanodiamonds is known from the analysis of meteors and lies in the region of 1.2-1.4 nm in diameter [3] Nanodiamonds possibly form in carbon stars and are emitted into the interstellar region by the star wind. The most favourable mechanism of their formation is through a collision process of carbon ions. During ejection from the carbon star and subsequent travel through the Universe, diamond nanoclusters undergo irradiation which causes their heating to a temperature whereby a transition from nanodiamond to carbon nanospiroid occurs as was shown in [3].

The transition to a spiroid form under irradiation is more likely than transition to a spheroid because these structures are less symmetric and can form from defective nanodiamonds more easily through radiation induced defects and skeleton strain [3].

Such structures that have been formed from nanodiamonds by irradiation have well defined optical properties which can act as their fingerprints. It is the optical properties of these irradiated structures that are the focus of this paper. I.e. in this paper we establish correlation between optical properties of carbon nano-spiroids, presenting in the interstellar medium and of 217.5 nm interstellar optical extinction band. Spectrum of this band is presented elsewhere (for the details of this band see, e.g., [4,5]). Optical absorption by carbon onions (multishell fullerenes) either synthesised in laboratory conditions [4] or possibly occurring naturally in the interstellar medium [4] has been modelled by different authors. In reference [2] calculations were performed in the framework of a nested spherical shells model. In this paper we establish correlation between optical properties of carbon nano-spheroids, possibly presenting in the interstellar medium and manifestation of 217.5 nm interstellar absorption (extinction) band. Spectrum of this band is presented elsewhere (for the details of this band see, e.g., [5,6]). We used model of homogeneous particle in electrostatic approximation [7] because formation of carbon nanospiroids accomplishes with some disorder that may softening the selection rules for radial tunneling of electrons and modify its workfunction. .

2 Results and discussion

2.1 The model

Density Functional Theory (DFT) *ab initio* studies by [8] have shown that the perpendicular to the graphene plane (out of the plane or perpendicular) component of the electric field does not noticeably introduce additional electrons into the conduction band of a graphene plane, in the spectral region (0 — $\sim$ 10 eV). For the component parallel to the graphene plane ("in plane" or tangential component), π electrons solely contribute to the optical properties in the $\hbar\omega \approx 4.5$—$\hbar\omega \approx 7$ eV spectral region (see [8]. By analogy with graphite the potential barrier for electrons is about the value of workfunction 4.6 eV (see, e.g. [9]). Analogously with graphene, similar components of the field will work similary for the case of carbon nano spheroid and nano spiroid, and the in plane component will fill up these particles with free electron gas when energy of photon is bigger than the workfunction value. The main difference between this paper and the work of [9] consists in the model of a carbon spiroid. In reference [10] the authors consider the onion as a multishell parti-

cle whose structure locally resembles graphite. They use both components of the dielectric tensor to explain the optical properties of a multishell fullerene. However, assuming presence of free electron gas in the cluster, it seems natural to use the model of a free electron gas filling an homogeneous sphere and the electrostatic approximation, for analysis of the optical absorption by carbon onions.

2.1.1 Optimisation of geometry of carbon nanospheroids and nanospiroids

Here we perform Car-Parrinello molecular dynamics geometry optimisation of $C_{60}@C_{240}$ carbon spheroid and C_{300} carbon spheroid and derived interatomic distance histograms for estimation of effect of disorder to the optical properties. In the studies of such complicated systems such as spheroids and spiroids, the knowledge of their morphology is essential for further calculations. Therefore, we have searched available data to develop models of the systems studied. Coordinates of carbon atoms for precursors of C_{300} spiroid, namely C_{60} fullerene (internal shell) and C_{240} (external shell), were collected from the internet site [10]. Algorithm of breeding of C_{60} and C_{240} double-shell spheroid in C_{300} spiroid has been adopted from [11]. The resulting $C_{60}@C_{240}$ multiwall fullerene (spheroid) and C_{300} spiroid are shown in Fig.1(a) and Fig.1(b), respectively. The mathematical model of such spiroid has been described in our earlier articles [13],[3],[14], and the graphical image of it is presented in Fig.1(c). As one can see, spiroid and spheroid (carbon onion) exhibit differences in their geometries. The characteristic feature of the spiroid is the opening hole with a well-seen passage that constitutes a quasi two-dimensional channel that ends up in the spiroids center of mass. Measurements have shown that the width of the entrance hole attains 9.3 Å, while the spacing between the adjacent shells within the channel varies from 2.8 Å at the edge to 3.6 Å in the middle of the channel. Geometries of spheroid and spiroid, as described above, have been optimized first by Avogadro molecular editor with UFF model [16] before they have been input to Car-Parrinello molecular dynamics (CPMD) code [16] with Nose thermostat [17], where the final optimization of geometry has been performed. Shapes of spiroid and spheroid after the resulting optimization of the geometry do not differ substantially from the ones presented in Fig.1. Considering other details of the computational CPMD procedure, we would like to mention that for all cases presented in this paper we considered a plane wave basis set with a cutoff of 50 Ry and the PBE exchange-correlation potential. The long-range van der Waals interaction has been accounted for by means of a semi-empirical DFT-D2 approach proposed by Grimme [18].

2.1.2 Statistics

Figures 2 and 3 show distribution of interatomic distances for carbon spheroid and spiroid presented in Fig.1, correspondingly. It is seen that for the case of spheroid the carbon skeleton for the latest one seems to be slightly distorted, or amorphised. Amorphisation in its turn may results in simplifying picture of optical transitions expecting for electrons because of breaking of the selection rules for the optical transitions for electrons (see, e.g. [20]) and, in our case,for radial tunnelling, because of local symmetry distorsions and two-dimensional geometry alteration. However, the total number of electrons participating in transition does not change owing to the conservation law for number of electrons bondind carbon atoms in the spiroidal cluster. One may suppose that both topological alterations of the surface of spiroid together with breaking of the selection rules may cause reduction of the work function downing the value 4.6 eV

2.2 The formalism

We shall start from the dielectric function ϵ of free electron gas [6]:

$$\epsilon_1 = \epsilon_\infty - \frac{\omega_\pi^2}{\omega^2 + \gamma^2} \tag{1}$$

$$\epsilon_2 = \frac{\omega_\pi^2 \gamma}{\omega(\omega^2 + \gamma^2)} \tag{2}$$

$$\epsilon_\infty = \frac{\omega_\pi^2}{\omega_\pi^2 + \gamma^2} \tag{3}$$

$$\epsilon = \epsilon_1 - i\epsilon_2 \tag{4}$$

here $\gamma = \frac{1}{\tau}$ is the inverse relaxation time ϵ_1 and ϵ_2 are the real and imaginary parts of the dielectric function, ω is frequency of photon, and the complex dielectric function of free electron gas is ϵ.

The polarisability of a vacuum-suspended spherical particle containing damped electron gas α with radius R obeys the equation [6]:

$$\alpha = R^3 \frac{\epsilon - 1}{\epsilon + 2} \tag{5}$$

Substituting ϵ with real and imaginary parts defined by (1–4) into equation (5), gives:

$$Re(i\alpha) = R^3 \frac{3\epsilon_2}{\epsilon_2^2 + (2+\epsilon_1)^2} \tag{6}$$

Optical extinction of an ensemble of spherical particles in the Rayleigh-Gans model is determined through the extinction cross section calculated for the single particle multiplied by the number of scatterers per unit volume ([6]). It is known that the optical extinction cross section Q_r induced by an ensemble of M equivalent vacuum-suspended single particles having a size much smaller than the wavelength of the radiation obeys the following expression ([6]):

$$Q_r = M 4\pi k Re(i\alpha) \tag{7}$$

where $k = \frac{2\pi}{\lambda}$ is wavenumber for a wave of wavelength λ; α is the polarisability of an extincting globular particle suspended in vacuo ([6]). Taking into account equations (6) and (7), gives:

$$Q_(r) = 12\pi \frac{\omega}{c} R^3 \frac{\epsilon_2}{\epsilon_2^2 + (2+\epsilon_\infty)^2} \tag{8}$$

We omitted here the number of particles M because of the normalised units available for experimental and interstellar extinction profiles. For correction of the monotonic trend in the interstellar extinction associated with extinction by silicate grains, we use the polynomial

$$Q_r' = \delta_0 + \delta_1\omega + \delta_2\omega^2 + \delta_3\omega^3$$

addition to equation (8). This form is termed by us as "the baseline".

It is easy to demonstrate that keeping assumption $\omega\tau \gg 1$, equation (8) attains its maximal value for the frequency of the Fröhlich resonance ω_{dF}:

$$\omega_{dF} = \frac{\omega_\pi}{(3+\epsilon_\infty)^{\frac{1}{2}}} \tag{9}$$

In this model of a free electron gas only the spiroid's outer border controls the free path of electrons, bouncing them backwards inside the sphere. Consequently, the relaxation time τ of free electrons confined in onions might be associated with the scattering of electrons by the outer shell and thus the classical free path effect model may be used. This states that if the particle radius R becomes less than the mean free path of an electron in a bulk material, l_∞, the interactions of the conduction electrons with the particle surface

become important as an additional collision process resulting in a reduced effective mean free path that is equal to R. This results in an increased ratio $\frac{1}{\tau(R)}$ which now depends on the particle radius:

$$\frac{1}{\tau(R)} = \frac{1}{\tau_0} + \frac{Av_{fe}}{R} \tag{10}$$

where v_{Fe} is the velocity of electrons at the Fermi level, $\frac{1}{\tau_0} = \frac{Av_{Fe}}{l_\infty}$; A includes details of the scattering process (see [21]) and is approximately unity.

2.3 The numerical fitting

For simultaneous estimation of the relaxation time and the plasma frequency, equation (8) was fitted to the literature [1] data that are portrayed with solid grey circles in Fig.4. The result of the fit is presented in Fig.**??** by the solid line with parameters given in the figure caption. A good agreement is seen in Fig.4 between the fit and digitised data over most of the spectral region.

The mean literature interstellar extinction curve is represented by the open circles in Fig.5. For estimation of the model parameters equation (8) with added baseline polynomial was fitted to the literature data. The results of the fit are shown by the solid full lines and fitting parameters values are presented in the figures captions.

3 Conclusions

The model of Fröhlich resonance applied to carbon onions fits reasonably well the experimental absorption spectrum together with the mean interstellar extinction curve, in the area where the prominent optical absorption 217.5 nm band becomes dominant. The results evidence on possibility of delocalisation of π electrons of carbon spiroids in its volume after irradiation by light.Such behaviour of electrons may results from a partial amorphisation of spiroid backbone atoms.

References

[1] Guillois O., Ledoux G, Reynaud C. The Astrophys. J. 521 (1999) L133L36

[2] Grill ., Pate V. Appl. Phys. Lett. 60 (1992) 2089

[3] Yastrebov S.G., Smith R., Siklitskaya A.V., Mont.Not.R.Astron. Soc. , 409, (2010) 1577

[4] Chhowalla M., Wang H., Sano N., Teo K.B.K., Lee S.B., Amaratunga G.A.J. Phys. Rev. Lett. 90 (2003) 155504

[5] Fitzpatrick E.L., Massa D.L. ApJS, 72 (1990) 163

[6] Fitzpatrick E.L. Publ. Astron. Pacific, 111, (1999) 63

[7] Bohren C.F., Huffman D.R., 1998, Absorption and scattering of light by small particles, Wiley, New York.

[8] Marinopoulos A. G., Reining L., Rubio A., Olevano V. Phys.Rev.B 69 (2004) 245419-1

[9] Krisenan K.S. Nat 26 (1952) 703

[10] Lucas A.A., Henrard L., Lambin Ph. Phys. Rev. B, 49 (1994) 2888

[11] Structural information about fullerene isomers. URL http://www.nanotube.msu.edu/fullerene/fullerene-isomers.html—¿15

[12] Ozawa M., Goto H., Kusunoki M., Osawa E. Journ.Phys.Chem.B. 106(2002) 7135

[13] Yastrebov S., Siklitskaya A., Smith R. Diamond Relat. Mater. 32 (2013) 32

[14] Yastrebov S., Siklitskaya A., Smith R. J. Appl.Phys. 114(2013) 134305 - 134305

[15] Hanwell, Marcus D; Curtis, Donald E; Lonie, David C; Vandermeersch, Tim; Zurek, Eva; Hutchison, Geoffrey R., J. Cheminform. 4(2012) 1-17.

[16] Car R.,Parrinello M. Phys. Rev. Lett. 55(1985) 2471

[17] Nos S., J. Chem. Phys., 81(1984) 511

[18] S. Grimme, J. Comput. Chem. 27(2006) 1787

[19] P. O. Bedolla, G. Feldbauer, M. Wolloch, S. J. Eder, N. Drr, P. Mohn, J. Redinger, A. Vernes, J. Phys. Chem. C Nanomater Interfaces. 118 31(2014) 1760817615

[20] Mott N.E., Davis A.F. Electronic Processes in Non-crystalline Materials Clarendon Press 1971

[21] Hövel H., Fritz S., Hilger A., Kreibig U., Vollmer M., 1993, Phys.Rev.B, 48, 18178

4 Figure captions

Fig.1 (color online) (a) Example of the multishell fullerene C300-carbon onion; (b) Typical spiroid obtained as a combination of C60 and C240 fullerenes (as described in the text); (c) Mathematical model of the spiroid (see the detailed description in the text). The spheres indicate atoms and sticks chemical bonds between carbon atoms. Green color indicates the edge of spiroids entrance.

Fig.2 Hystogram of interatomic distances between ajacent carbon atoms for multishell spheroid presented in Fig.1, left panel.

Fig.3 Hystogram of interatomic distances between ajacent carbon atoms for spiroid presented in Fig.1, central panel.

Fig. 4: The optical extinction cross-section for carbon onions as a function of photon energy. The grey circles are the experiment results for carbon onions presented by [4]. The full line corresponds to the best fit of equation (8) to the experimental data (with outliers omitted) for the following set of parameters: ϵ_∞=1.432, $\hbar\omega_\pi$=10.405±0.03 eV, $\frac{\tau}{\hbar}$=0.562±0.02. eV^{-1}

Fig. 5: Fragment of the mean interstellar extinction profile [5,6], represented by circles. The solid full line corresponds to the best fit of equation (8) to the data for the following set of parameters: ϵ_∞=1.432, $\hbar\omega_\pi$=10.43±0.001 eV, $\frac{\tau}{\hbar}$=0.797±0.001, eV^{-1}. The thin line portrays the polynomial baseline. The dashed line shows the residual between the original profile and the restored baseline with parameters: δ_0=0, δ_1=0.874, δ_2=-0.084, δ_3=0.00377 in normalised units.

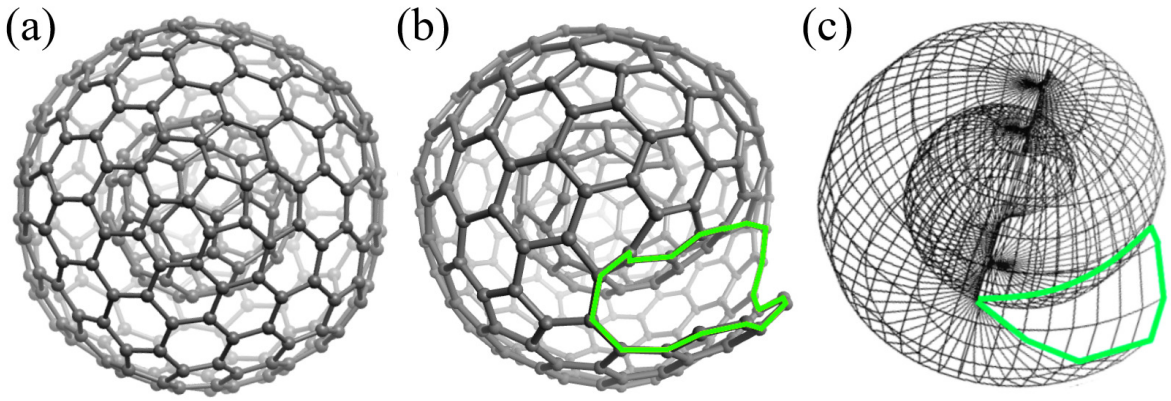
(a)
(b)
(c)

Fig. 1.

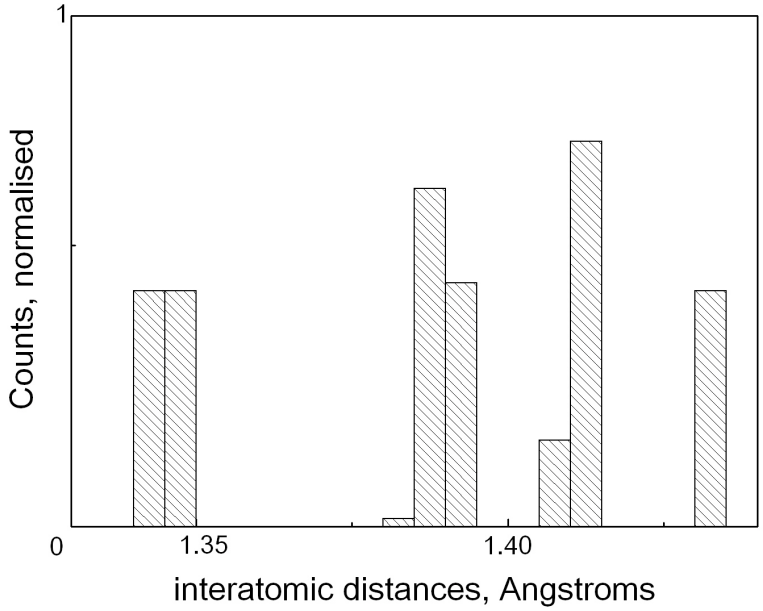
1
0
1.35
1.40
Counts, normalised
interatomic distances, Angstroms

Fig. 2.

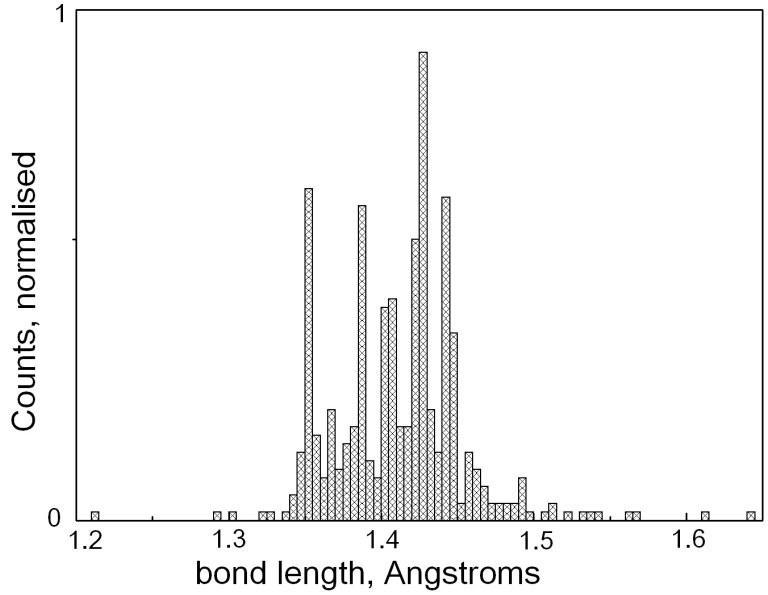

Fig. 3.

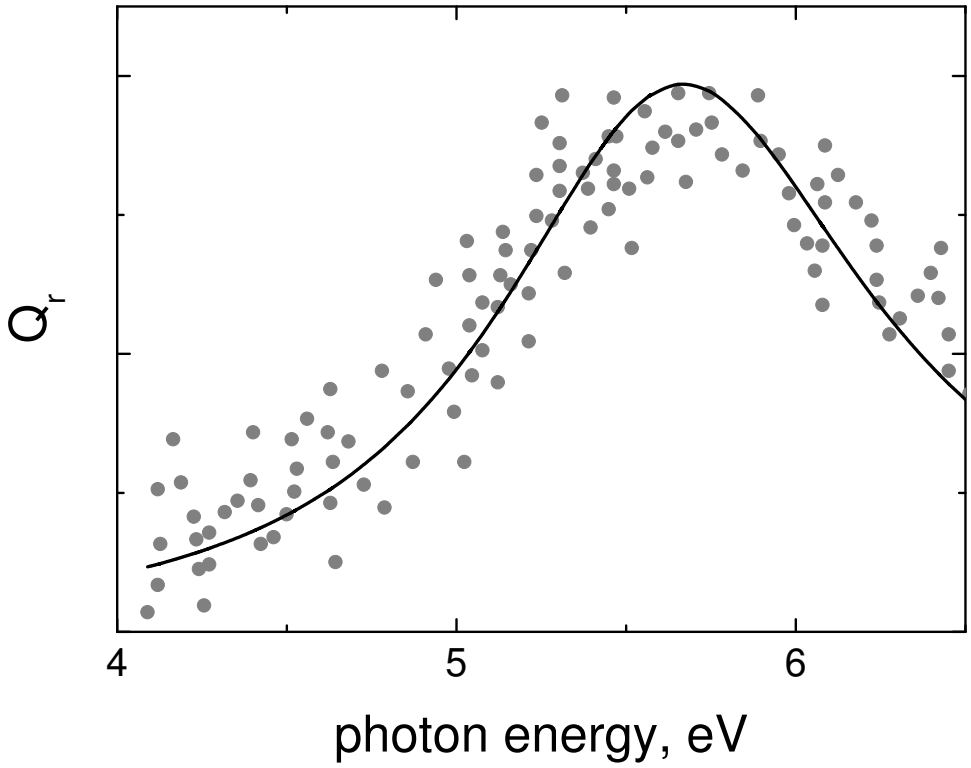

Fig. 4.

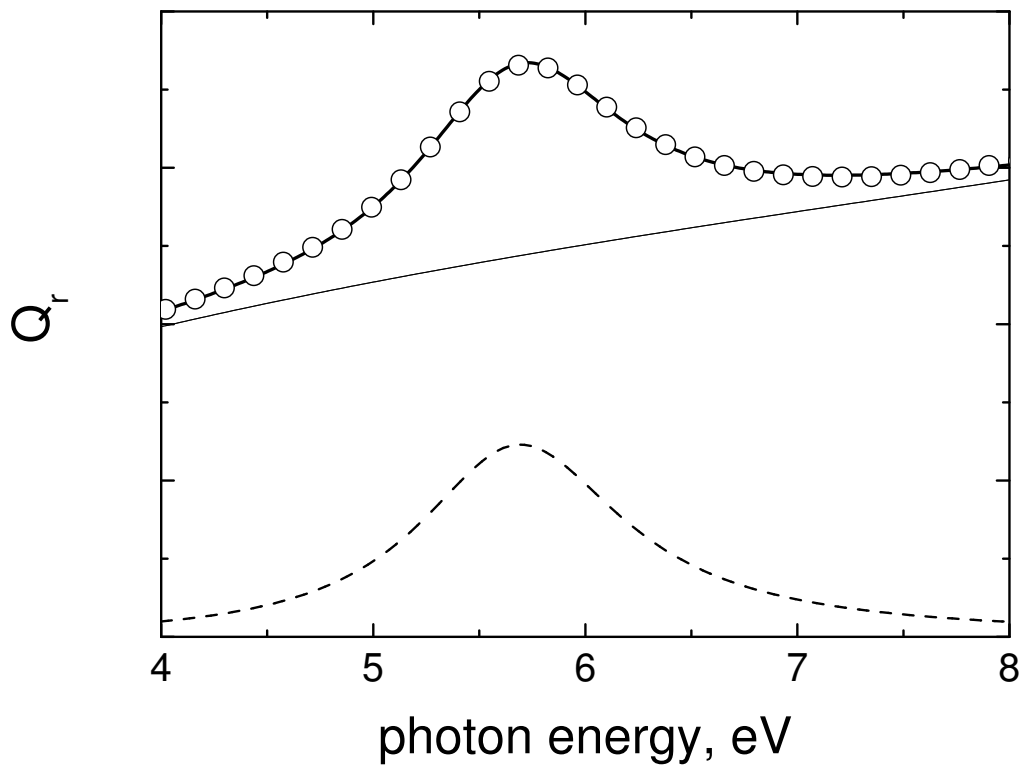

Fig. 5.